The Effects of Probe-Induced Flow Distortion on Atmospheric Turbulence Measurements

J. C. WYNGAARD

National Center for Atmospheric Research[1], Boulder, CO 80307

(Manuscript received 20 January 1981)

ABSTRACT

We present a theory for probe-induced flow distortion which is applicable in the atmosphere at heights greater than about 10 times the obstacle size. We use the theory to calculate the behavior of Reynolds shear stress and velocity variances ahead of a cylinder and a sphere. The stress is found to be most seriously distorted, the extent depending on the nature of the trailing wake. We show that the linear form of the theory should be adequate for most surface-layer applications, and we discuss how the theory can be applied to more complex geometries. We show that the "tilt correction" approach to the problem, which has been used by some workers, is incorrect in principle since it violates vorticity conservation, and is not even a good approximation in general.

1. Introduction

The masts and instrument mounts used by micrometeorologists inevitably cause distortion of the flow being measured. This distortion is most evident in the mean velocity field; for example, upwind of an obstacle the mean streamwise wind component is attenuated, a lateral mean wind is induced, and often a mean vertical velocity is detectable as well. Aspects of the mean wind-field distortion near meteorological towers have been studied by Dabberdt (1968a,b), Camp and Kaufman (1970), Izumi and Barad (1970), Mollo-Christensen (1979), and Wucknitz (1980).

Surface-layer researchers are showing increasing concern about the effects of this mean-flow distortion on turbulent flux measurements, particularly on stress, a key parameter in surface-layer turbulence theory. In his paper discussing the flow distortion generated by an obstacle in a boundary layer, Mollo-Christensen (1979) states that ". . . one must also realize that large flux distortion can be induced by comparatively slight mean velocity disturbances, and that one must not only check the mean velocity distortion, but also the distortion of the flux field, for flux observation programs." Garratt (1979) and Schmitt *et al.* have exchanged comments on the possible influence of flow distortion on the Schmitt *et al.* (1978) stress measurements at 8 m height, 30 m upwind of a large offshore platform. Wieringa (1980) has claimed that the stresses measured in the 1968 Kansas experiments were seriously in error because of tower-induced mean flow distortion, and has proposed corrections to some of the surface-layer relations inferred from the Kansas data.

The theoretical framework for calculating the effects of mean-flow distortion on turbulence under typical surface-layer conditions is poorly developed. As a result, Wieringa (1980), for example, did not actually calculate from first principles the response of stress to the alleged mean flow distortion in the Kansas experiments. Instead, he simply assumed that the "tilt" equations, developed originally to predict the stress errors caused by instrument misalignment in an undistorted flow, also give the stress response to mean flow distortion. This amounts to assuming that the stress, measured in axes aligned with the local mean steamlines, is unchanged by the flow distortion.

In this paper we develop a theory for mean-flow distortion effects on turbulence structure when the turbulence integral scale is much larger than the obstacle, as is typical of probe-induced distortion in the surface layer. We present detailed calculations of the distortion of stress and velocity variances upwind of a two-dimensional circular cylinder and a sphere under typical surface layer conditions, and find that the tilt equations are not correct in this application.

[1] The National Center for Atmospheric Research is sponsored by the National Science Foundation.

0021-8952/81/070784-11$06.75

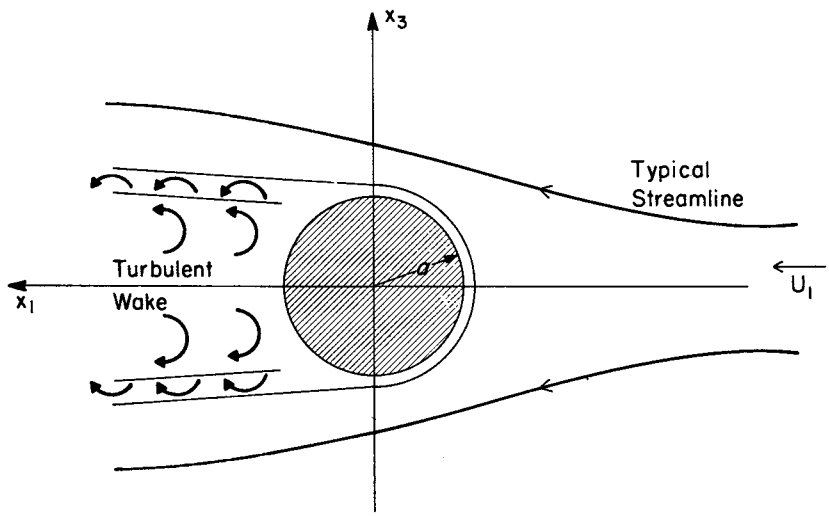

FIG. 1. A representation of the flow past a circular cylinder (from Hunt, 1973).

2. A theory for mean-flow distortion effects on very large-scale turbulence

To illustrate the problem, Fig. 1 shows a two-dimensional cylinder of radius a inserted in a turbulent flow of integral scale L_x, velocity scale q, shearing stress $\overline{u_1u_3}$ and mean velocity $U_i = [U_1(x_3), 0, 0]$. The upstream extent of the mean streamline distortion caused by the cylinder scales with a, and we wish to know how $\overline{u_1u_3}$ and the velocity variances are distorted from their free-stream values in this region. We do not restrict our approach to cylinders, however, and in the arguments to follow a denotes a characteristic length of the body.

Hunt (1973) has presented a lengthy and intricate analysis of a simpler problem: weak, isotropic turbulence in a uniform stream approaching a circular cylinder. Using the linearized vorticity equation, Hunt finds that the mean distortion effects on the turbulent velocity variances are quite different in the limits $a/L_x \gg 1$ and $a/L_x \ll 1$.

We will consider only the case $a/L_x \ll 1$, and show that this is typically satisfied for probe-induced flow distortion in the atmospheric surface layer. The approach we develop for this limit need not be restricted to weak, isotropic turbulence, but instead can treat an oncoming flow with large turbulence level, mean shear, and turbulent stress.

We now show that if $a/L_x \ll 1$, the effect of mean shear, turbulent shear, and time changes in the oncoming flow can be neglected. Taking mean shear first, we note that in a neutral surface layer $\partial U_1/\partial z = u_* k^{-1} z^{-1}$, $U_1 = u_* \ln(z/z_0)k^{-1}$, in standard notation. Near the surface $L_x \approx z$ for vertical wind fluctuations (Kaimal *et al.*, 1972); L_x for horizontal wind fluctuations under unstable conditions is much larger (Kaimal, 1978). The change in free-stream mean velocity ΔU_1 over the height of the body is of order $a\partial U_1/\partial z$, and thus $\Delta U_1/U_1 \approx a(z \ln z/z_0)^{-1} \approx a(L_x \ln z/z_0)^{-1}$. Thus $\Delta U_1/U_1 \ll 1$ if $a/L_x \ll 1$. It follows that we can neglect the mean wind shear in the limit $a/L_x \ll 1$, since it implies that over distances of the order of the body size the mean free-stream flow is effectively uniform (Van Dyke, 1964).

The oncoming flow also has turbulent shear and thus turbulent vorticity. The turbulent vorticity in the free-stream flow has a three-dimensional wavenumber spectrum proportional to $\epsilon^{2/3}\kappa^{1/3}$ in the inertial range; it peaks near the Kolmogorov wavenumber $(\epsilon/\nu_3)^{1/4}$ and falls sharply at higher wavenumbers (Tennekes and Lumley, 1972). By integrating this spectral form we see that the rms turbulent vorticity carried by eddies of wavenumber smaller than a^{-1} is of order $\epsilon^{1/3}a^{-2/3}$. Since ϵ is of order q^3/L_x, this free-stream turbulent vorticity is of order $qL_x^{-1/3}a^{-2/3}$. In order that we be able to neglect this, we require that the velocity perturbation induced ahead of the body by this free-stream vorticity perturbation be small compared with the velocity perturbation induced by the free-stream velocity perturbation. For a cylinder, Van Dyke (1964) discusses the velocity field induced by free-stream vorticity, and his results indicate that our requirement is met if the free-stream turbulent vorticity is small compared to q/a, which is true if $(a/L_x)^{1/3} \ll 1$.

The temporal changes in the free-stream flow have a time scale L_x/q. We require that this time scale be much larger than the time scale for flow adjustment around the body, which is of order a/U. This is equivalent to requiring that $L_x/a \gg q/U$, which is met if $a/L_x \ll 1$.

Thus when $a/L_x \ll 1$, the free-stream flow has

negligible spatial variations (i.e., is irrotational) and is quasi-steady. We denote this undistorted, far upstream flow (equivalently, the flow which would exist in the absence of the body) by $\mathcal{U}_i = U_i + u_i = (U_1 + u_1, u_2, u_3)$; here U_1 is the undistorted mean flow, aligned with the x_1 axis, and $u_i = (u_1, u_2, u_3) = u_i(t)$ is the undistorted turbulent flow. We denote the distorted velocity field upstream of the body with a tilde: $\tilde{\mathcal{U}}_i = \tilde{U}_i + \tilde{u}_i = (\tilde{U}_1 + \tilde{u}_1, \tilde{U}_2 + \tilde{u}_2, \tilde{U}_3 + \tilde{u}_3)$. Even though the undistorted mean velocity field is purely in the x_1 direction, the distorted mean field will have at least two nonzero components.

Our solution will involve a series expansion about the mean flow state. This general approach has been used successfully in a variety of related problems; for example, Rose (1962) used it to find expressions for the directional sensitivity of hot-wire arrays, and Wyngaard *et al.* (1974) (see also Wyngaard, 1981) have used it to derive a differential equation describing cup anemometer dynamics.

We assume that the distorted flow field upstream of the body is an analytic function of the undistorted oncoming flow, i.e.,

$$\tilde{\mathcal{U}}_i = \tilde{U}_i + \tilde{u}_i = \tilde{\mathcal{U}}_i[\mathbf{x}, U_1 + u_1(t), u_2(t), u_3(t)]. \quad (1)$$

We expand $\tilde{\mathcal{U}}_i$ in a Taylor series about the unidirectional upstream flow, neglecting terms of second and higher order in the free-stream turbulence

$$\tilde{\mathcal{U}}_i \approx \tilde{\mathcal{U}}_i(\mathbf{x}, U_1, 0, 0) + a_{i1}(\mathbf{x})u_1(t) + a_{i2}(\mathbf{x})u_2(t) + a_{i3}(\mathbf{x})u_3(t),$$

$$a_{ij}(\mathbf{x}) = \frac{\partial \tilde{\mathcal{U}}_i(\mathbf{x})}{\partial \mathcal{U}_j}\bigg|_0. \quad (2)$$

The subscript zero means evaluated at the basic, unidirectional state. In this Taylor series representation of $\tilde{\mathcal{U}}_i$, the only random variables are the free-stream turbulence components $u_i(t)$; the leading term in (2) is simply the steady flow response, and the coefficients $a_{ij}(\mathbf{x})$ are nonrandom functions which depend on $\mathbf{x}$ and on the body shape.

When (2) is averaged the terms involving $u_i(t)$ vanish and the expression for the distorted mean flow becomes simply

$$\overline{\tilde{\mathcal{U}}_i} = \tilde{U}_i \approx \tilde{U}_i(\mathbf{x}, U_1, 0, 0). \quad (3)$$

Eq. (3) reveals that the mean flow ahead of the body is, to first order in the upstream turbulence level, simply the flow which would exist in response to a nonturbulent free stream. Subtracting (3) from (2) gives an expression for the distorted turbulence field,

$$\tilde{u}_i(\mathbf{x}, t) \approx a_{i1}(\mathbf{x})u_1(t) + a_{i2}(\mathbf{x})u_2(t) + a_{i3}(\mathbf{x})u_3(t), \quad (4)$$

where again we have neglected terms of second and higher order.

In the absence of the body the coefficients a_{ij} in (2) and (4) become δ_{ij}, the Kronecker delta, and (4) reduces to $\tilde{u}_i(\mathbf{x}, t) = u_i(t)$. In general, however, the a_{ij} differ from δ_{ij}, so the flow distortion introduces "crosstalk" among the turbulence components.

The crosstalk coefficients a_{ij} in (2) and (4) can be calculated analytically from the solution for potential flow about the body. In the next three sections we demonstrate this calculation for a two-dimensional circular cylinder and a sphere.

3. Large-scale turbulence upstream of a circular cylinder

We will evaluate the coefficients $a_{ij}(\mathbf{x}) = \partial \tilde{\mathcal{U}}_i(\mathbf{x})/\partial \mathcal{U}_j\big|_o$ upstream of a circular cylinder of radius a, as sketched in Fig. 1. The undisturbed, far upstream flow has a mean velocity $U_1(x_3)$ directed along the x_1 axis and a Reynolds shear stress $\overline{u_1 u_3}$. L_x, the scale of the mean shear and of the energy-containing eddies, is much larger than a.

The velocity potential ϕ for this flow is

$$\phi = -\mathcal{U}_1 x_1(1 + a^2/r^2),$$

where $r^2 = x_1^2 + x_3^2$. The distorted velocity components are

$$\left.\begin{aligned} \tilde{\mathcal{U}}_1 &= \frac{-\partial\phi}{\partial x_1} = \mathcal{U}_1\left[1 + \frac{a^2}{r^2}\left(1 - \frac{2x_1^2}{r^2}\right)\right] \\ \tilde{\mathcal{U}}_3 &= \frac{-\partial\phi}{\partial x_3} = -\frac{2\mathcal{U}_1 a^2 x_1 x_3}{r^4} \end{aligned}\right\}. \quad (6)$$

From (6) we have immediately

$$\left.\begin{aligned} a_{11}(\mathbf{x}) &= \frac{\partial \tilde{\mathcal{U}}_1(\mathbf{x})}{\partial \mathcal{U}_1}\bigg|_0 = \frac{\tilde{\mathcal{U}}_1(\mathbf{x})}{\mathcal{U}_1}\bigg|_0 \\ a_{31}(\mathbf{x}) &= \frac{\partial \tilde{\mathcal{U}}_3(\mathbf{x})}{\partial \mathcal{U}_1}\bigg|_0 = \frac{\tilde{\mathcal{U}}_3(\mathbf{x})}{\mathcal{U}_1}\bigg|_0 \end{aligned}\right\}. \quad (7)$$

Furthermore, from the symmetry of the flow with respect to x_2 we have $a_{i2}(\mathbf{x}) = 0$.

To calculate $a_{i3}(\mathbf{x})$ we consider an arbitrary point P ahead of the cylinder (Fig. 2) and let the free-stream flow have an infinitesimal lateral component $d\mathcal{U}_3$. Then due to the circular symmetry the new distorted flow components are still represented by (6) if we rotate the coordinate system through an angle $d\alpha = d\mathcal{U}_3/\mathcal{U}_1$. We denote with a prime components measured in this rotated system. Thus in the presence of a free-stream component $d\mathcal{U}_3$, the

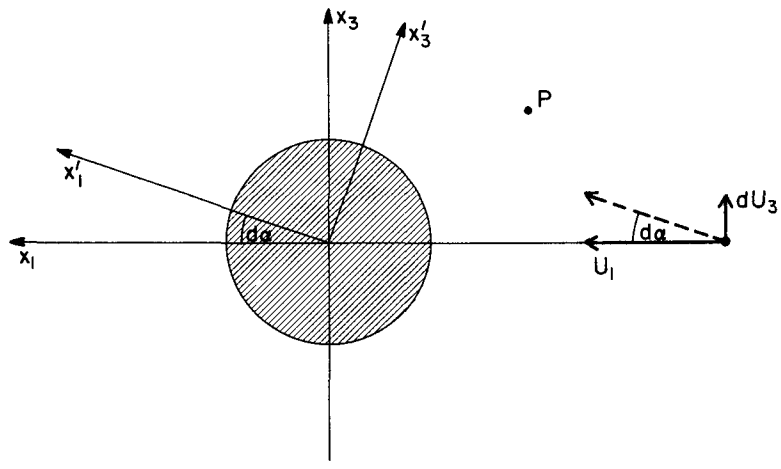

FIG. 2. When the flow approaches the circular cylinder at an angle $d\alpha$ to the x_1-axis, the velocity at point P can be calculated from the velocity potential by rotating the axes through $d\alpha$.

velocity components at P are, in the rotated coordinates,

$$\left.\begin{aligned}(\tilde{U}_1 + d\tilde{U}_1)' &= \tilde{U}_1 + \frac{\partial \tilde{U}_1}{\partial x_1} \times (x_1' - x_1) + \frac{\partial \tilde{U}_1}{\partial x_3}(x_3' - x_3) \\ (\tilde{U}_3 + d\tilde{U}_3)' &= \tilde{U}_3 + \frac{\partial \tilde{U}_3}{\partial x_1} \times (x_1' - x_1) + \frac{\partial \tilde{U}_3}{\partial x_3}(x_3' - x_3)\end{aligned}\right\}. \quad (8)$$

Using the relations $x_1' - x_1 = x_3 d\alpha, x_3' - x_3 = -x_1 d\alpha$ and calculating the derivatives in (8) from (6) then gives

$$\left.\begin{aligned}(\tilde{U}_1 + d\tilde{U}_1)' &= \tilde{U}_1 + 2\tilde{U}_3 d\alpha \\ (\tilde{U}_3 + d\tilde{U}_3)' &= \tilde{U}_3 + 2(U_1 - \tilde{U}_1)d\alpha\end{aligned}\right\}. \quad (9)$$

Transforming to the original coordinates, Eq. (9) becomes

$$\left.\begin{aligned}\tilde{U}_1 + d\tilde{U}_1 &= (\tilde{U}_1 + d\tilde{U}_1)' \cos(d\alpha) - (\tilde{U}_3 + d\tilde{U}_3)' \sin(d\alpha) = \tilde{U}_1 + \tilde{U}_3 d\alpha \\ \tilde{U}_3 + d\tilde{U}_3 &= (\tilde{U}_3 + d\tilde{U}_3)' \cos(d\alpha) + (\tilde{U}_1 + d\tilde{U}_1)' \sin(d\alpha) \\ &= \tilde{U}_3 + (2U_1 - \tilde{U}_1)d\alpha\end{aligned}\right\}. \quad (10)$$

Thus from (10) we have

$$\left.\begin{aligned}d\tilde{U}_1 &= \tilde{U}_3 d\alpha \\ d\tilde{U}_3 &= (2U_1 - \tilde{U}_1)d\alpha\end{aligned}\right\}. \quad (11)$$

Finally, using $d\alpha = d\tilde{U}_3/\tilde{U}_1$ yields

$$\left.\begin{aligned}a_{13}(\mathbf{x}) &= \frac{\partial \tilde{U}_1(\mathbf{x})}{\partial U_3}\bigg|_0 = \frac{\tilde{U}_3(\mathbf{x})}{U_1}\bigg|_0 \\ a_{33}(\mathbf{x}) &= \frac{\partial \tilde{U}_3(\mathbf{x})}{\partial U_3}\bigg|_0 = 2 - \frac{\tilde{U}_1(\mathbf{x})}{U_1}\bigg|_0\end{aligned}\right\}. \quad (12)$$

In view of (3), we can write the a_{ij} results (7) and (12) as

$$\left.\begin{aligned}a_{11}(\mathbf{x}) &= \frac{\tilde{U}_1(\mathbf{x})}{U_1} \\ a_{31}(\mathbf{x}) &= \frac{\tilde{U}_3(\mathbf{x})}{U_1} = a_{13}(\mathbf{x}) \\ a_{33}(\mathbf{x}) &= 2 - \frac{\tilde{U}_1(\mathbf{x})}{U_1}\end{aligned}\right\}, \quad (13)$$

where the distorted mean flow components $\tilde{U}_1$ and $\tilde{U}_3$ are, from (3) and (6),

$$\left.\begin{aligned}\tilde{U}_1 &\approx U_1\left[1 + \frac{a^2}{r^2}\left(1 - \frac{2x_1^2}{r^2}\right)\right] \\ \tilde{U}_3 &\approx -2U_1 \frac{a^2 x_1 x_3}{r^4}\end{aligned}\right\}. \quad (14)$$

Having found the a_{ij}, we can now use (4) and write expressions for the distorted turbulence components upstream of the cylinder as

$$\left.\begin{aligned}\tilde{u}_1(\mathbf{x}, t) &\approx \frac{\tilde{U}_1(\mathbf{x})}{U_1} u_1(t) + \frac{\tilde{U}_3(\mathbf{x})}{U_1} u_3(t) \\ \tilde{u}_3(\mathbf{x}, t) &\approx \frac{\tilde{U}_3(\mathbf{x})}{U_1} u_1(t) + \left[2 - \frac{\tilde{U}_1(\mathbf{x})}{U_1}\right] u_3(t)\end{aligned}\right\}. \quad (15)$$

to first order in the turbulence level. Using (6) and (8) allows us to write (15) in the form

$$\left.\begin{aligned}\tilde{u}_1 &= u_1 + 2\frac{a^2}{r^2}\left[\left(\frac{1}{2}-\frac{x_1^2}{r^2}\right)u_1 - \frac{x_1x_3}{r^2}u_3\right]\\ \tilde{u}_3 &= u_3 - 2\frac{a^2}{r^2}\left[\left(\frac{1}{2}-\frac{x_1^2}{r^2}\right)u_3 + \frac{x_1x_3}{r^2}u_1\right]\end{aligned}\right\}. \quad (16)$$

This form shows that the contamination effects decay as $(a/r)^2$ away from the cylinder.

Squaring and averaging each of (15) gives expressions for the distorted variance and stress

$$\overline{\tilde{u}_1^2} = \left(\frac{\tilde{U}_1}{U_1}\right)^2\overline{u_1^2} + \frac{2\tilde{U}_1\tilde{U}_3}{U_1^2}\overline{u_1u_3} + \left(\frac{\tilde{U}_3}{U_1}\right)^2\overline{u_3^2},$$

$$\overline{\tilde{u}_3^2} = \left(\frac{\tilde{U}_3}{U_1}\right)^2\overline{u_1^2} + 2\frac{\tilde{U}_3}{U_1}\left(2-\frac{\tilde{U}_1}{U_1}\right) \times \overline{u_1u_3} + \left(2-\frac{\tilde{U}_1}{U_1}\right)^2\overline{u_3^2},$$

$$\overline{\tilde{u}_1\tilde{u}_3} = \frac{\tilde{U}_1\tilde{U}_3}{U_1^2}\overline{u_1^2} + \left[\left(\frac{\tilde{U}_3}{U_1}\right)^2 + \left(2-\frac{\tilde{U}_1}{U_1}\right)\frac{\tilde{U}_1}{U_1}\right] \times \overline{u_1u_3} + \overline{u_3^2}\frac{\tilde{U}_3}{U_1}\left(2-\frac{\tilde{U}_1}{U_1}\right). \quad (17)$$

On the stagnation line ($\theta = \pi$), and at $\theta = \pi/2$ the results (17) can be compared with Hunt's (1973) calculations. There $\tilde{U}_3 = 0$, from (14), and we have

$$\left.\begin{aligned}\overline{u_1^2} &= \left(\frac{\tilde{U}_1}{U_1}\right)^2\overline{u_1^2}\\ \overline{u_3^2} &= \left(2-\frac{\tilde{U}_1}{U_1}\right)^2\overline{u_3^2}\end{aligned}\right\}. \quad (18)$$

Figs. 8, 10, 12, and 15 of Britter *et al.* (1979) show that (18) agrees with the calculations of Hunt (1973) in the limit $a/L_x \to 0$.

We can present (17) in compact graphical form if we define a parameter $R_{\alpha\beta}(\mathbf{x})$, the ratio of $\overline{\tilde{u}_\alpha\tilde{u}_\beta}$ in the distorted flow upstream of the body to its undistorted, far upstream value:

$$R_{\alpha\beta}(\mathbf{x}) = \frac{\overline{\tilde{u}_\alpha\tilde{u}_\beta}(\mathbf{x})}{\overline{u_\alpha u_\beta}}. \quad (19)$$

Figs. 3 and 4 show contours of constant R_{13}, R_{11} and R_{33} upstream of the cylinder. Fig. 3a is for $\overline{u_1^2}/u_*^2 = 5.3$, $\overline{u_3^2}/u_*^2 = 1.7$, where $u_*^2 = -\overline{u_1u_3}$; these conditions are typical of the stable or near-neutral surface layer. Fig. 3b has $\overline{u_1^2}/u_*^2 = 9$, $\overline{u_3^2}/u_*^2 = 4$, typical of the very unstable surface layer. Notice that the stress $\overline{u_1u_3}$ is reduced in the region below the cylinder center plane, and increased in the region above; the effects are stronger under very unstable conditions. The plots for R_{11} look qualitatively like those for R_{33}, but different from R_{13}; the principal difference between the R_{11} and R_{33} plots is that the regions of amplification and attenuation are interchanged. In general, the effects on $\overline{u_1^2}$ and $\overline{u_3^3}$ are less severe than those on $\overline{u_1u_3}$, and the effects on all three quantities increase with increasing turbulence level.

4. Large-scale turbulence upstream of a sphere

We use the geometry of Fig. 1, except that we place a sphere of radius a at the origin. The procedure just used for the cylinder gives the following linear contributions to the distorted turbulent velocity field:

$$\left.\begin{aligned}\tilde{u}_1(\mathbf{x},t) &= u_1(t) + \frac{3}{2}\frac{a^3}{r^3}\left[\left(\frac{1}{3}-\frac{x_1^2}{r^2}\right)u_1(t) - \frac{x_1x_2}{r^2}u_2(t) - \frac{x_1x_3}{r^2}u_3(t)\right]\\ \tilde{u}_2(\mathbf{x},t) &= u_2(t) + \frac{3}{2}\frac{a^3}{r^3}\left[-\frac{x_1x_2}{r^2}u_1(t) + \left(\frac{1}{3}-\frac{x_2^2}{r^2}\right)u_2(t) - \frac{x_2x_3}{r^2}u_3(t)\right]\\ \tilde{u}_3(\mathbf{x},t) &= u_3(t) + \frac{3}{2}\frac{a^3}{r^3}\left[-\frac{x_1x_3}{r^2}u_1(t) - \frac{x_2x_3}{r^2}u_2(t) + \left(\frac{1}{3}-\frac{x_3^2}{r^2}\right)u_3(t)\right]\end{aligned}\right\}. \quad (20)$$

The distorted mean flow components are

$$\left.\begin{aligned}\tilde{U}_1(\mathbf{x}) &= U_1\left(1 + \frac{a^3}{2r^3} - \frac{3}{2}x_1^2\frac{a^3}{r^5}\right)\\ \tilde{U}_2(\mathbf{x}) &= U_1\left(-\frac{3}{2}x_1x_2\frac{a^3}{r^5}\right)\\ \tilde{U}_3(\mathbf{x}) &= U_1\left(-\frac{3}{2}x_1x_3\frac{a^3}{r^5}\right)\end{aligned}\right\}. \quad (21)$$

In this case the coefficients in the expressions (20) for the distorted turbulence components cannot be expressed simply in terms of the distorted mean field, as was possible in Eq. (15) for flow ahead of the cylinder.

There are two additional features of (20) worth emphasizing. One is the $(a/r)^3$ dependence of the contamination terms, indicating faster decay than for the two-dimensional cylinder. Second, the flow distortion contaminates each of the three turbulent

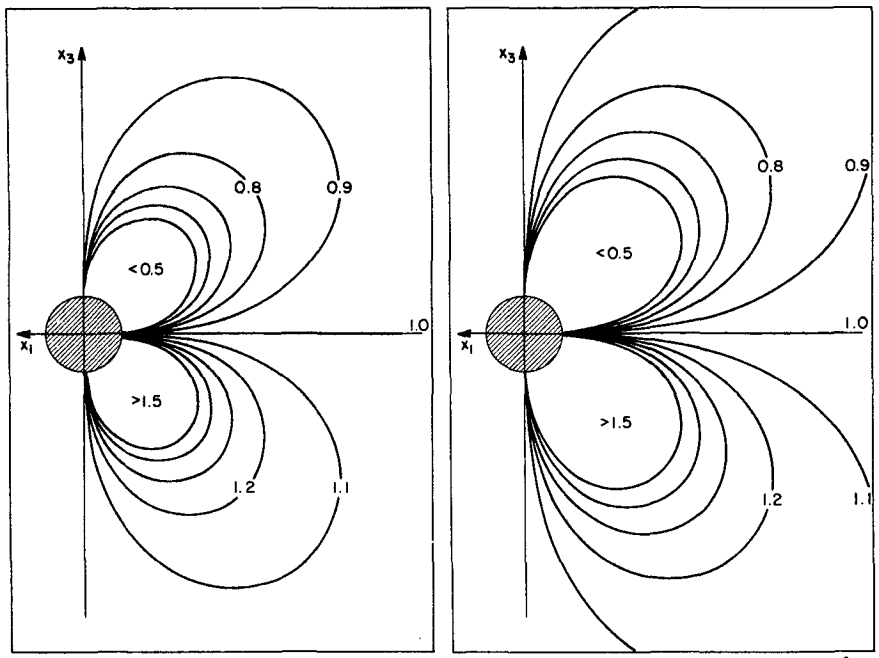

FIG. 3. Contours of R_{13} upstream of a wakeless circular cylinder. Left: $\overline{u_1^2}/u_*^2 = 5.3$, $\overline{u_3^2}/u_*^2 = 1.7$. Right: $\overline{u_1^2}/u_*^2 = 9$, $\overline{u_3^2}/u_*^2 = 4$.

velocity components with the other two, in contrast to the two-dimensional case where there is no contamination of or by the axial component.

Fig. 5 shows some calculations of $R_{\alpha\beta}$ ahead of the sphere in the $x_2 = 0$ plane. The $R_{\alpha\beta}$ results are similar to those for the cylinder, Figs. 3 and 4, but the distortion effects decay more rapidly away from the sphere.

5. Wake effects

In Sections 3 and 4 we used the classical results for potential flow around a cylinder and a sphere in our solution for mean distortion effects on turbulence. In practice, a cylinder, sphere, or other bluff body in large Reynolds number flow creates a turbulent wake. In this section we investigate the effects of this wake on the upstream turbulence.

We will use the model of a circular cylinder and its wake described by Wucknitz (1980). The model includes an approaching parallel flow of velocity U_1, a source of Q of strength $2U_1y_1$ at the origin, and, at a distance $a/2$ downstream, a sink S of smaller strength $-2U_1y_2$. The complex potential is

$$w(z) = \phi + i\chi = -U_1 \times \left[z + \frac{y_1}{\pi} \ln z - \frac{y_2}{\pi} \ln(z - a/2) \right], \quad (22)$$

where $z = x_1 + ix_3$. The contour of the body simulating the cylinder of radius a and its wake is

$$x_3 + \frac{y_1}{\pi} \arctan\left(\frac{x_3}{x_1}\right) - \frac{y_2}{\pi} \times \arctan\left(\frac{x_3}{x_1 - a/2}\right) + y_2 - y_1 = 0. \quad (23)$$

It follows from (23) that the wake half-width approaches $y_1 - y_2$ as $x_1 \to \infty$. Wucknitz (1980) shows that in real flows one expects values of dimensionless wake width $C_D = (y_1 - y_2)/a$ ranging from 0.3 to 1.2, depending on the Reynolds number. Fixing C_D fixes one of the two parameters y_1 and y_2 in terms of the other; the remaining one can then be varied to make the upstream body contour approach a circular arc of radius a. We achieved this over the range $0.25 \leq C_D \leq 1.25$ by choosing $y_1/a = 6.5 - 2.0C_D$. The resulting contours of cylinder and wake are shown for several C_D values in Fig. 6.

To apply our approach to flow about the contours in Fig. 6, we need the velocity potential for upstream flow approaching at an arbitrary angle to the x_1 axis. In our cylinder and sphere calculations in Sections 3 and 4, their symmetry made one potential applicable for all approach angles. Fortunately this is the case here as well, since only the circular leading edge of the contours in Fig. 6 represents the body. The downstream contours simulate the wake edges, which will rotate about the x_2 axis as the flow approach angle varies, remaining parallel to the oncoming flow. This assumes that the time changes

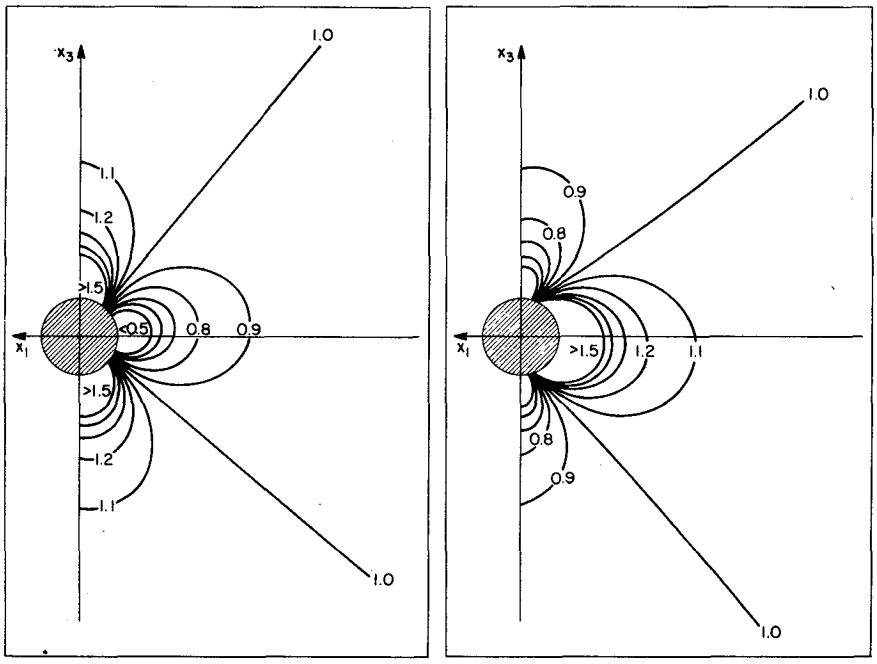

FIG. 4. Contours of R_{11} (left) and R_{33} (right) ahead of a wakeless circular cylinder for $\overline{u_1^2}/u_*^2 = 5.3$, $\overline{u_3^2}/u_*^2 = 1.7$.

in the approach flow are slow enough, which is the case for $a/L_x \ll 1$.

Thus the potential (22) can be used with our calculation method to find the distortion of large-scale turbulence upstream of a cylinder with a realistic wake. For a cylinder center located at $(a/4, 0)$ we find

$$\left.\begin{aligned} a_{11} &= \tilde{U}_1/U_1; \quad a_{31} = \tilde{U}_3/U_1; \\ a_{13} &= \frac{ax_3}{2\pi}\left[\frac{y_2(a/2 - x_1)}{r_2^4} - \frac{y_1 x_1}{r^4}\right] \\ a_{33} &= 1 + \frac{ay_2}{4\pi r_2^2}\left(1 - \frac{2x_3^2}{r_2^2}\right) \\ &\quad + \frac{ay_1}{4\pi r^2}\left(1 - \frac{2x_3^2}{r^2}\right) \end{aligned}\right\}, \quad (24)$$

where $r_2^2 = (x_1 - a/2)^2 + x_3^2$. The distorted mean velocity components are

$$\left.\begin{aligned} \tilde{U}_1 &= U_1\left[1 + \frac{y_1 x_1}{\pi r^2} - \frac{y_2(x_1 - a/2)}{\pi r_2^2}\right] \\ \tilde{U}_3 &= \frac{U_1 x_3}{\pi}\left[\frac{y_1}{r^2} - \frac{y_2}{r_2^2}\right] \end{aligned}\right\}. \quad (25)$$

Eqs. (24) and (25) in conjunction with (4) enable us to generate equations for the distorted variances and stress as was done in section 3 for the wakeless cylinder. Fig. 7 shows the resulting contours of R_{13} upstream of a circular cylinder for $C_D = 0.5$ and $C_D = 1.0$, which as shown in Fig. 6 have wake widths equal to the cylinder radius and cylinder diameter, respectively. A comparison with the wakeless cylinder results, Fig. 3, shows that the principal effects of the wake are felt above and below the cylinder, i.e., near $x_1 = 0$. There the wakeless potential flow is nearly parallel to the x_1 axis, while the presence of the wake generates a significant $\tilde{U}_3$ value there. Thus without a wake R_{13} approaches 1.0 there, while with a wake R_{13} is significantly less than 1.0 above the cylinder and greater than 1.0 below it.

6. The tilt correction

Some authors have suggested that mean flow distortion effects on turbulent velocity components can be removed through the tilt corrections normally used (Deacon, 1969; Kaimal and Haugen, 1969; Hyson *et al.*, 1977) to correct for instrument misalignment or tilt. Thus if α is the angle between the x_1 axis and the tangent to the local mean streamline, the distorted turbulent velocity components in this hypothesis are, for a two-dimensional flow,

$$\left.\begin{aligned} \tilde{u}_1 &= u_1 \cos\alpha + u_3 \sin\alpha \\ \tilde{u}_3 &= -u_1 \sin\alpha + u_3 \cos\alpha \end{aligned}\right\}. \quad (26)$$

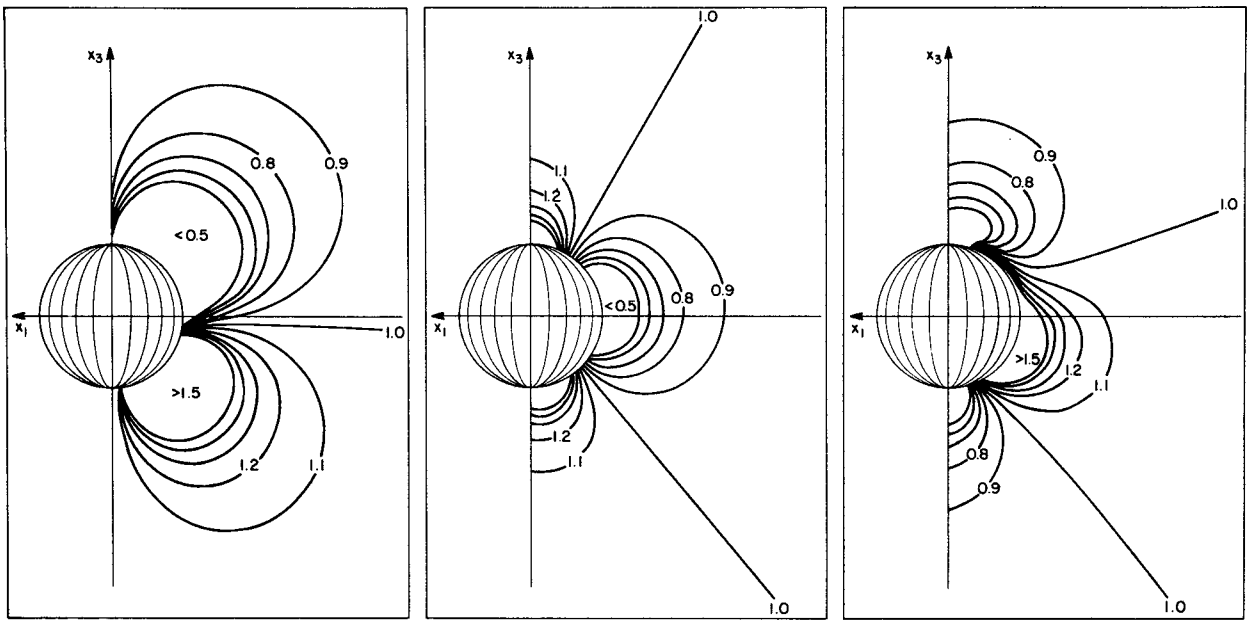

FIG. 5. Contours of R_{13} (left), R_{11} (center), and R_{33} (right) on the center plane ahead of a wakeless sphere for $\overline{u_1^2}/u_*^2 = 5.3$, $\overline{u_3^2}/u_*^2 = 1.7$.

Note that our results [e.g., Eq. (15) for the wake-free case and (24) and (25) with a wake, are not of the form (26)].

We can prove that the tilt hypothesis (26) for flow distortion is incorrect. Let the undistorted, upstream u_i field be irrotational. Then since molecular diffusion effects are negligible ahead of the body in the large Reynolds number flows we are considering, the distorted field must also be irrotational. Thus the x_2 vorticity component $\tilde{u}_{1,3} - \tilde{u}_{3,1}$ must vanish. From (26) this implies that

$$\frac{\partial \alpha}{\partial x_1}(u_1 \cos\alpha + u_3 \sin\alpha) + \frac{\partial \alpha}{\partial x_3}(u_3 \cos\alpha - u_1 \sin\alpha) = 0. \quad (27)$$

For (27) to hold for arbitrary magnitudes of u_1 and u_3 it is necessary that $\partial\alpha/\partial x_1 = \partial\alpha/\partial x_3 = 0$. This is true only if the distorted streamlines are parallel, which is not the case ahead of a body. Thus the tilt model (26) does not conserve vorticity, and similar arguments show that it also does not conserve mass. Thus "tilt corrections" for mean flow distortion effects are incorrect in general.

We can assess the stress errors introduced by assuming the tilt correction (26) holds for flow around a cylinder. If (26) were true, then the effects of flow distortion could be removed by defining tilt-corrected components through

$$\left.\begin{aligned} u_1^t &= \tilde{u}_1 \cos\alpha - \tilde{u}_3 \sin\alpha \\ u_3^t &= \tilde{u}_1 \sin\alpha + \tilde{u}_3 \cos\alpha \end{aligned}\right\}, \quad (28)$$

since (26) and (28) together imply that $u_1^t = u_1$, $u_3^t = u_3$, and hence that $\overline{u_1^t u_3^t} = \overline{u_1 u_3}$. Our expressions (26) and (24) for distortion allow us to calculate the ratio of tilt-corrected and undistorted stress,

$$T(\mathbf{x}) = \overline{u_1^t u_3^t}(\mathbf{x})/\overline{u_1 u_3}. \quad (29)$$

Fig. 8 shows the T results for flow about a cylinder. By comparing it with Figs. 3 and 7 we see that the

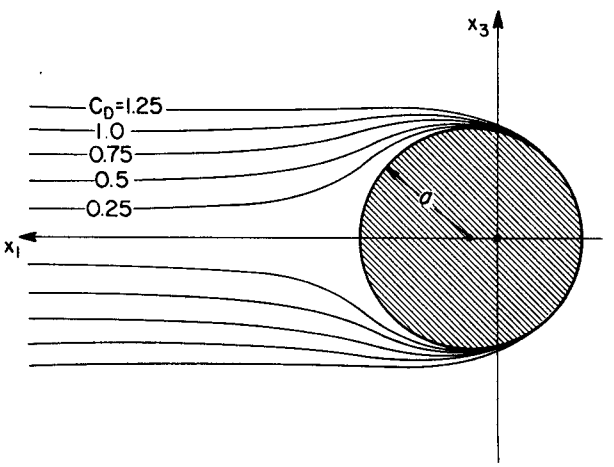

FIG. 6. The contours of a circular cylinder and its wake as described by the Wucknitz model [Eq. (23)] for various C_D values.

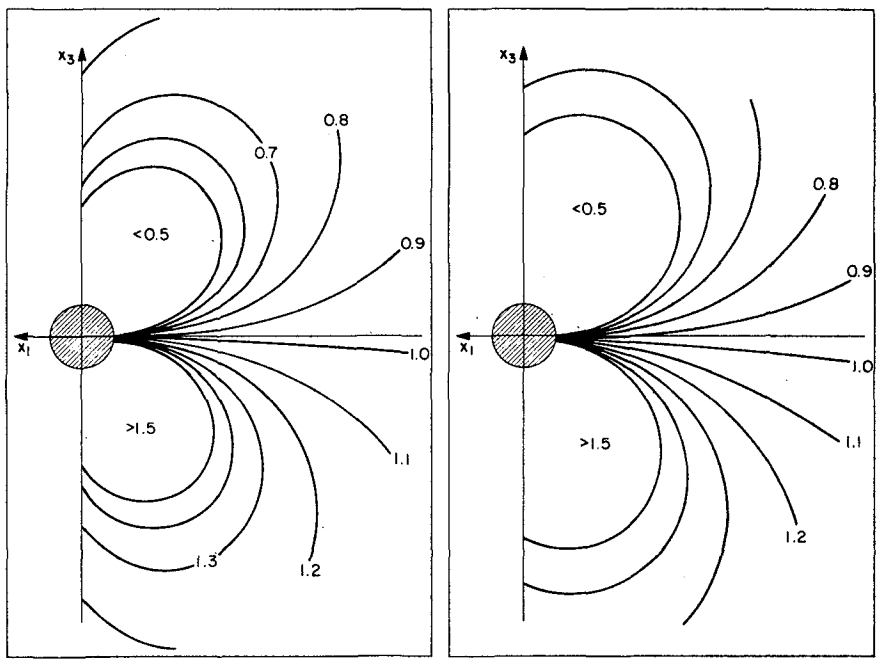

FIG. 7. Contours of R_{13} upstream of a circular cylinder for $\overline{u_1^2}/u_*^2 = 9$, $\overline{u_3^2}/u_*^2 = 4$, with a wake. Left, $C_D = 0.5$; right, $C_D = 1.0$.

tilt correction restores about half the distortion-induced stress error, both with and without a wake present.

7. Applications to micrometeorology

There are several points to be discussed regarding the application of our theory to the flow distortion problems met in micrometerological measurements.

a. The assumption $L_x \gg a$

We have assumed that the turbulence integral scale L_x is much larger than the obstacle length scale a. Britter *et al.* (1979), who made laboratory measurements of the distortion of weak turbulence by a circular cylinder, found that the effects were quite different for $a/L_x \gg 1$ and $a/L_x \ll 1$; for example, they found that $\overline{\tilde{u}_1^2}$ on the stagnation line was attenuated for $a/L_x \ll 1$ but amplified for $a/L_x \gg 1$, as predicted by Hunt (1973). They used a/L_x values as small as 0.11, and while it is not clear from their results that the $\tilde{u}_1$ and $\tilde{u}_3$ components approach the $a/L_x = 0$ predictions at the same rate, it seems that a/L_x values of the order of 0.1 or less are needed. Applications to the unstable atmospheric surface layer are complicated by the existence of much different L_x values for the horizontal components u_1 and u_2 than for u_3. The Kansas and Minnesota results Kaimal, 1978) indicate that $L_x \simeq 1.0z$ for u_3, and hence we suggest that our approach be restricted to cases with $a < 0.1z$.

b. Second-order effects

Our calculations to this point have used only the linear terms in the Taylor series expansion (2) of the distorted velocity field. The next-order terms involve the coefficients.

$$b_{ijk}(\mathbf{x}) = \frac{\partial^2 \tilde{\mathcal{U}}_i(\mathbf{x})}{\partial \mathcal{U}_j \partial \mathcal{U}_k}\bigg|_0 = b_{ikj}(\mathbf{x}) \tag{30}$$

of which there are six different ones for each i. However, $b_{i11} = 0$ because $\tilde{\mathcal{U}}_i$ is linear in $\mathcal{U}_1$. Further, if either j or k is 1, b_{ijk} also vanishes by the following argument. On dimensional grounds, $\partial \tilde{\mathcal{U}}_i(\mathbf{x})/\partial \mathcal{U}_k$ can be written as $f_{ik}(\mathbf{x}/a, \alpha_k)$ where $\alpha_k = \mathcal{U}_k/\mathcal{U}_1$ and f_{ik} depends on the body shape. Since $\partial/\partial \mathcal{U}_1 = -(\alpha_j/\mathcal{U}_1)\partial/\partial\alpha_j$, we have

$$\frac{\partial^2 \tilde{\mathcal{U}}_i(\mathbf{x})}{\partial \mathcal{U}_1 \partial \mathcal{U}_k} = -\frac{\alpha_j}{\mathcal{U}_1}\frac{\partial f_{ik}}{\partial \alpha_j}. \tag{31}$$

Evaluating (31) at $\alpha_j = 0$ then shows that $b_{i1k} = 0$. Thus in the general two-dimensional case only b_{i33} is non-zero.

For the special case of a wakeless circular cylinder it is found that b_{i33} vanishes, but in the general two-dimensional case the equations for the distorted mean and turbulence become, through second order,

$$\tilde{U}_i = \tilde{U}_i(\mathbf{x}, U_1, 0, 0) + \tfrac{1}{2} b_{i33}\overline{u_3^2}, \tag{32}$$

$$\tilde{u}_i = a_{i1}u_1 + a_{i2}u_2 + a_{i3}u_3 + \tfrac{1}{2}b_{i33}(u_3^2 - \overline{u_3^2}). \tag{33}$$

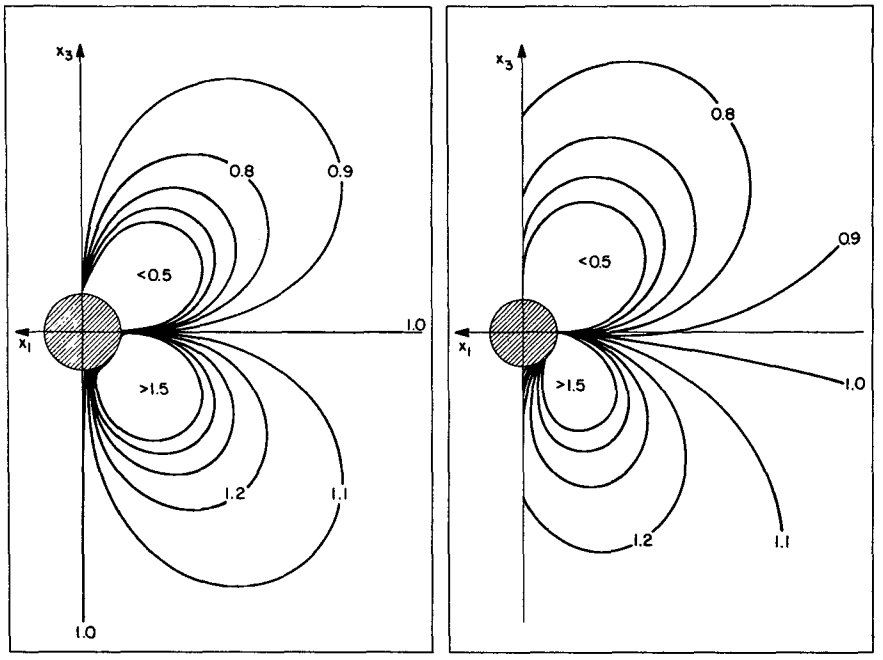

FIG. 8. Contours of T, the ratio of tilt corrected and undistorted $\overline{u_1 u_3}$, upstream of a circular cylinder for $\overline{u_1^2}/u_*^2 = 9$, $\overline{u_3^2}/u_*^2 = 4$. Left, wakeless; right, wake with $C_D = 1.0$.

Eq. (32) says that there are differences, of second order in the turbulence level, between the mean velocity and the steady potential flow solution. Eq. (33) says that there is nonlinear contamination of the turbulence components, in addition to the linear crosstalk. These nonlinear effects are apt to be small, however, since even under convective conditions $\overline{u_\alpha^2}/U_1^2$ does not normally exceed 0.10 for $\alpha = 1$, 2 or 3. Thus we conclude that our linear approximation is satisfactory under typical surface-layer conditions.

c. *Other body shapes*

We used a sphere and a circular cylinder to demonstrate our approach, but real flow-distortion problems are apt to involve more complex shapes. An aircraft fuselage, for example, can cause flow-distortion effects on turbulence measured from forward-pointing booms; a balloon can distort measurements from the tethering cable below; and typical fast-response micrometeorological anemometers can cause flow distortion through their bulky housings and mounts.

At first glance the aircraft and balloon problems may not seem more complex, since there are classical potential flow solutions for bodies resembling them. However, these classical solutions are not directly useful because they assume approach flow along the axis of the body, while our technique requires the solution for flow at an arbitrary angle to the axis. There are analytical techniques for generating such solutions, and these would be worth exploring.

Very complex and irregular shapes, such as anenometer mounts and housings, might best be treated in a different way. Rather than calculating the crosstalk coefficients $a_{ij}(\mathbf{x})$ analytically, as we have done here, one might measure them experimentally. The definition (2) of $a_{ij}(\mathbf{x})$ suggests how this could be done. One would measure (in a wind tunnel, say) the distorted velocity field $\tilde{\mathcal{U}}_i(\mathbf{x})$ ahead of a model of the body as a function of the free-stream velocity $\mathcal{U}_j$, and then determine $a_{ij}(\mathbf{x})$ from $\partial\tilde{\mathcal{U}}_i(\mathbf{x})/\partial\mathcal{U}_j$ evaluated at the basic state. An analogous technique was successfully used by Wyngaard *et al.* (1974) to measure coefficients in a differential equation for cup-anemometer response, as discussed by Wyngaard (1981).

8. Summary

Our theory should be useful in the probe-induced turbulence distortion problems in micrometeorology, providing the scale of the distorting body is less than about one-tenth the distance above the surface. The linear form of the theory should be adequate, since second-order effects are shown to be generally small in the surface layer.

We have shown through sample calculations that stress can be distorted quite severely ahead of a circular cylinder or a sphere. The presence of a

wake behind the body also influences the nature of the stress distortions.

Finally, we have shown that the "tilt corrections" used by some workers to correct for flow distortion effects on turbulence are incorrect in principle, since they violate conservation of vorticity. They are shown not to be even a good approximation in general.

Acknowledgments. I am grateful to J. Wieringa for bringing my attention to the problem through his 1980 BLM paper; to J. Garratt, for many subsequent discussions about micrometeorological flow distortion; to R. Rotunno, for discussions about the potential flow calculations; to R. Meitín, who skillfully prepared computer plots of the results; and to D. Howard, who cheerfully and tirelessly typed several versions of the manuscript.

REFERENCES

Britter, R. E., J. C. R. Hunt and J. C. Mumford, 1979: The distortion of turbulence by a circular cylinder. *J. Fluid Mech.*, **92**, 269–301.

Camp, D. W., and J. W. Kaufman, 1970: Comparison of tower influence on wind velocity for NASA's 150-meter meteorological tower and a wind tunnel model of the tower. *J. Geophys. Res.*, **75**, 1117–1121.

Dabberdt, W. F., 1968a: Tower-induced errors in wind profile measurements. *J. Appl. Meteor.*, **7**, 359–366.

——, 1968b: Wind disturbance by a vertical cylinder in the atmospheric surface layer. *J. Appl. Meteor.*, **7**, 367–371.

Deacon, E. L., 1969: The levelling error in Reynolds' stress measurement. *Bull. Amer. Meteor. Soc.*, **49**, 836.

Garratt, J. R., 1979: Comments on "Sea surface stress measurements," by Schmitt *et al.* (1978). *Bound.-Layer Meteor.*, **17**, 269–271.

Hunt, J. C. R., 1973: A theory of turbulent flow round two-dimensional bluff bodies. *J. Fluid Mech.*, **61**, 625–706.

Hyson, P., J. R., Garratt and R. J. Francey, 1977: Algebraic and electronic correction of measured *uw* covariance in the lower atmosphere. *J. Appl. Meteor.*, **16**, 43–47.

Izumi, Y., and M. L. Barad, 1970: Wind speeds as measured by cup and sonic anemometers and influenced by tower structure. *J. Appl. Meteor.*, **9**, 851–856.

Kaimal, J. C., 1978: Horizontal velocity spectra in an unstable surface layer. *J. Atmos. Sci.*, **35**, 18–24.

——, and D. A. Haugen, 1969: Some errors in the measurements of Reynolds stress. *J. Appl. Meteor.*, **8**, 460–462.

——, J. C. Wyngaard, Y. Izumi and O. R. Coté, 1972: Spectral characteristics of surface-layer turbulence. *Quart. J. Roy. Meteor. Soc.*, **98**, 563–589.

Mollo-Christensen, E., 1979: Upwind distortion due to probe support in boundary layer observation. *J. Appl. Meteor.*, **18**, 367–370.

Rose, W. G., 1962: Some corrections to the linearized response of a constant-temperature hot-wire anemometer operated in a low-speed flow. *Trans. ASME, J. Appl. Mech.*, **84**, 554–558.

Schmitt, K. F., C. A. Friehe and C. H. Gibson, 1978: Sea-surface stress measurements. *Bound.-Layer Meteor.*, **15**, 215–228.

——, ——, and ——, 1979: Reply. *Bound.-Layer Meteor.*, **17**, 273–274.

Tennekes, H., and J. L. Lumley, 1972: *A First Course in Turbulence*. The MIT Press, 300 pp.

Van Dyke, M., 1964: *Perturbation Methods in Fluid Mechanics*. Academic Press, 229 pp.

Wieringa, J., 1980: A reevaluation of the Kansas mast influence on measurements of stress and cup anemometer overspeeding. *Bound.-Layer Meteor.*, **18**, 411–430.

Wucknitz, J., 1980: Flow distortion by supporting structures. *Air-Sea Interaction, Instruments and Methods*, F. Dobson and L. Hasse, Eds., Plenum Press, 815 pp. (see pp. 605–626).

Wyngaard, J. C., 1981: Cup, propeller, vane, and sonic anemometers in turbulence research. *Annual Review of Fluid Mechanics*, Vol. 13, Annual Reviews, Inc., 399–423.

——, J. T. Bauman and R. A. Lynch, 1974: Cup anemometer dynamics. *Flow—Its Measurement and Control in Science and Industry*, Vol. 1, Instrum. Soc. Amer., 701–708.